J|A|C|S
COMMUNICATIONS

Published on Web 12/19/2006

Chiral Cyanide-Bridged $Mn^{II}Mn^{III}$ Ferrimagnets, $[Mn^{II}(HL)(H_2O)][Mn^{III}(CN)_6]\cdot 2H_2O$ (L = *S*- or *R*-1,2-diaminopropane): Syntheses, Structures, and Magnetic Behaviors

Wakako Kaneko, Susumu Kitagawa,* and Masaaki Ohba*

Department of Synthetic Chemistry and Biological Chemistry, Graduate School of Engineering, Kyoto University, Katsura, Nishikyo-ku, Kyoto 615-8510, Japan

Received August 24, 2006; E-mail: ohba@sbchem.kyoto-u.ac.jp

Chirality is one of the significant properties of molecules and plays a vital role inside the living body, which is deeply related to the origin of life. At the same time, chirality is also an important key factor for exhibiting specific physical properties, for example, second harmonic generation (SHG), magneto-chiral dichroism (MChD), ferroelectricity, etc.[1−3] Chirality can be controlled at the molecular level and can be installed into solid-state materials as a factor to cause crystal anisotropy based on the noncentrosymmetric molecular arrangements. Recently, several magnets providing noncentrosymmetric structures have been prepared by the use of optically active organic co-ligands.[4−8] Such magnets are promising compounds of multifunctionalities. However, in most cases, the structural chirality did not sufficiently relate to the magnetic properties, most likely because of the isotropic electron configurations of the constituents. It is a valuable approach to incorporate a single-ion magnetic anisotropy to the chiral frameworks for improving the correlation between the chirality and the magnetic properties through Dyaloshinkii−Moriya interaction. Here we report syntheses, structures, and magnetic properties of enantiomeric 2-D cyanide-bridged mixed-valence $Mn^{II}Mn^{III}$ assemblies $[Mn^{II}(HL)(H_2O)][Mn^{III}(CN)_6]\cdot 2H_2O$ (L = *S*- or *R*-1,2-diaminopropane (*S*-pn (**1S**) or *R*-pn (**1R**)) and the related racemic compound (L = *rac*-pn (**1rac**)).

Compounds **1S** and **1R** were obtained as dark-red crystals by the reaction of $MnCl_2\cdot 4H_2O$, L·2HCl, KOH, and $K_3[Mn(CN)_6]$ in the 1:3:5:1 molar ratio.[9] To avoid the oxidation and decomposition of $[Mn(CN)_6]^{3-}$, all the operations for the synthesis are carried out in a deoxygenated aqueous solution with cooling and light shielding. Both compounds showed two ν(C≡N) bands at 2140 and 2129 cm^{-1}, indicating the existence of bridging and terminal cyanide groups in the lattice.

The X-ray single-crystal structural analyses revealed that **1S** and **1R** are enantiomers.[10] The asymmetric unit consists of one $[Mn^{II}(HL)(H_2O)]^{2+}$ cation, one $[Mn^{III}(CN)_6]^{3-}$ anion, and lattice water molecules (Figure S1). $[Mn^{III}(CN)_6]^{3-}$ coordinates to the adjacent Mn^{II} ions in equatorial-μ^4-bridging mode. The Mn^{II} ion is in a pseudo-octahedral geometry with four cyanide nitrogen atoms (N1, N2, N5, and N6) in the equatorial positions, one amino nitrogen atom (N7) of HL, and one water oxygen atom (O1) at the axial positions. The terminal amino group (N8) of L is protonated, and the other amino group (N7) is coordinated to the Mn^{II} ion as a cationic monodentate ligand. In the lattice, a 2-D grid sheet structure is formed on the *ab* plane through $Mn^{III}-CN-Mn^{II}$ linkages (Figures 1 and S2). This structure is the same as that of $[Mn(HL)(H_2O)][Cr(CN)_6]\cdot H_2O$ except for the number of lattice water molecules.[5b] Compound **1rac** forms essentially same 2-D sheet structure as **1S** and **1R** with a slightly longer intersheet separation and centrosymmetric space group, $P2_1/m$.[11] Selected bond distances and angles are listed in Table S1 in the Supporting Information.

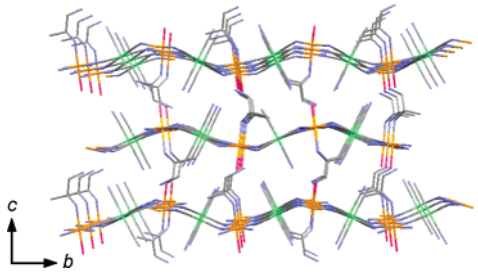

Figure 1. Projection onto the *bc* plane of **1S**. Atoms: Mn^{II} (Orange), Mn^{III} (green), N (blue), O (red), C (gray).

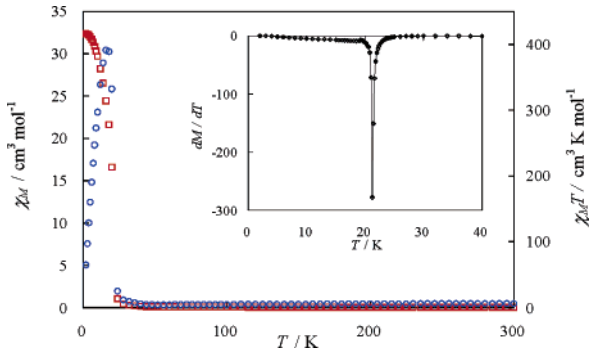

Figure 2. χ_M versus T (□) and $\chi_M T$ versus *T* (○) plots for **1S**. The inset is the d*M*/d*T* versus *T* plots using field-cooled-magnetization data.

The shortest intra- and intersheet $Mn^{II}\cdots Mn^{III}$ distances are 5.182(1) and 7.259(1) Å for **1S**, 5.167(1) and 7.267(1) Å for **1R**, and 5.224(1) and 7.513(1) Å for **1rac**, respectively.

The optical activity of compounds **1S** and **1R** were confirmed by solid-state CD spectra using a pressed KBr disk including 1% (w/w) of the samples in the range of 250−650 nm at 300 K (Figure S3). The respective spectrum patterns were inverted from each other with dominant bands around 270, 350, and 450 nm.[12] These results well reflect that the optical activity of these compounds originated from the chiral co-ligands.

Magnetic behaviors for polycrystalline **1S** and **1R** were almost the same. Reproducibility of all magnetic behaviors was confirmed with other samples prepared by other batches. The χ_M versus *T* and $\chi_M T$ versus *T* plots of **1S** under an applied field of 500 G are shown in Figure 2. The $\chi_M T$ value per $Mn^{II}Mn^{III}$ unit is 6.02 cm^3 K mol^{-1} (6.94 μ_B) at room temperature, which is well consistent with the spin-only value (5.38 cm^3 K mol^{-1}, 6.56 μ_B) expected for magnetically isolated Mn^{II} ($S = {}^5/_2$) and Mn^{III} ($S = {}^2/_2$) ions. The $\chi_M T$ value gradually decreases with lowering temperature down to the minimum value of 4.23 cm^3 K mol^{-1} at 56 K, then rapidly increases up to the maximum value of 390.9 cm^3 K mol^{-1} at 16 K. Below 16 K, $\chi_M T$ decreases down to 64.7 cm^3 K mol^{-1} (22.7 μ_B)

10.1021/ja066140b CCC: $37.00

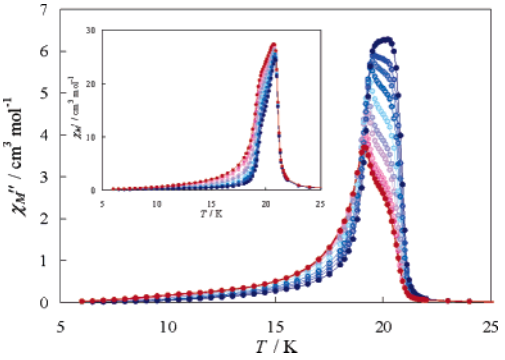

Figure 3. Temperature variation of the imaginary component of the ac magnetic susceptibility of **1S** at frequencies 1−1500 Hz (1 Hz, red circle; 1500 Hz, blue circle) under applied ac field of 3 G. The inset is that of the real component.

at 2 K because of the saturation of magnetization. The Curie−Weiss plot in the temperature ranges of 300 −100 K gives a Weiss constant θ of −56 K. The first decrease of $\chi_M T$ and the negative θ value suggest the operation of an antiferromagnetic interaction between the adjacent Mn^{II} and Mn^{III} ions through cyanide bridges and a small contribution of spin−orbit coupling of low-spin Mn^{III}. The magnetic phase transition temperatures (T_c) of both compounds were determined to be 21.2 K by weak-field magnetization measurements (Figures S5−7) and dM/dT plots (Figures 2 and S8). In the ac susceptibility under an ac magnetic field of 3 G, the in-phase signal (χ_M') and out-of phase signal (χ_M'') show a rapid increase below 21.2 K. The χ_M' versus T plot shows a peak at 20.8 K with a shoulder around 19.6 K with a frequency-dependence. Also the χ_M'' versus T plot shows a peak at 19.1 K with a shoulder around 20 K at 1 Hz, and the curve shape drastically changed with increase of frequency (Figures 3 and S9−10). The secondary peak of χ_M'' slightly shifts toward higher temperature ($\Delta T = 0.4$ K from 1 to 1500 Hz) upon increasing the frequency. Also a small magnetic anomaly was observed around 8 K in χ_M''. ZFCM and RM curves also indicate the two-step magnetic phase change. Such behaviors have not been observed in the $Mn^{II}Cr^{III}$ analogue, which suggests that they would originate from domain dynamics and spin reorientation which correlates with the magnetic anisotropy of Mn^{III} ion and chiral structure.

Magnetic hysteresis loops of **1S** and **1R** at 2 K are given in Figures S11−13. The saturation magnetization value per $Mn^{II}Mn^{III}$ unit at 50 kG is 3.12 (for **1S**) and 3.15 (for **1R**) $N\beta$ which corresponds to the value of $S = {}^3/_2$ expected for antiferromagnetically coupled Mn^{II} and Mn^{III} ions with an average g value of 2.12 and 2.14, respectively. Both coercive fields ($\mathbf{H}_c$) are determined to be 120 G, which is larger than that of the corresponding $Mn^{II}Cr^{III}$ analogue ($\mathbf{H}_c = 10$ G). The larger coercive field must be associated with the magnetic anisotropy of Mn^{III} ion. The shapes of the magnetic hysteresis loops strongly support the long-range ferrimagnetic ordering of **1S** and **1R**. Magnetic behaviors of **1rac** are essentially the same as **1S** and **1R** except for T_c (20.8 K), two minima in dM/dT versus T plot, no magnetic anomaly around 8 K in χ_M'', and large $\mathbf{H}_c$ (690 G).

Novel 2-D $Mn^{II}Mn^{III}$ ferrimagnets ($T_c = 21.2$ K), $[Mn(HL)(H_2O)]$-$Mn(CN)_6]\cdot 2H_2O$ (L = *S*-pn (**1S**), *R*-pn (**1R**), and *rac*-pn (**1rac**)) have been prepared. Compounds **1R** and **1S** are enantiomeric and crystallized in noncentrosymmetric space group $P2_12_12_1$. Simultaneously, they provide a mixed-valence metal combination (class I). The combination of chirality and mixed-valence is also expected to exhibit multifunctional properties. Both compounds successfully show an anomaly around 20 and 8 K in ac magnetic behaviors. The latter anomaly vanished in racemic compound **1rac**, which suggests a relation between magnetic structure and structural chirality. Detailed magnetic measurements with single crystals and other physical measurements are now in progress. Also we are promoting further systematic preparation of $Mn^{II}Mn^{III}$ compounds with other chiral and achiral co-ligands.

Acknowledgment. This work was supported by a Grant-In-Aid for Science Research in a Priority Area 'Chemistry of Coordination Space (No. 16074209)' from the Ministry of Education, Science, Sports and Culture, and Core Research for Evolutional Science and Technology (CREST), Japan Science and Technology Corporation (JST), Japan. W.K. is grateful to JSPS Research Fellowships for Young Scientists.

Supporting Information Available: Crystallographic data (CIF), CD spectra, and magnetic data of **1S**, **1R**, and **1rac**. This material is available free of charge via the Internet at http://pubs.acs.org.

References

(1) (a) Lacroix, P. G.; Clément, R.; Nakatani, K.; Zyss, J.; Ledoux, I. *Science* **1994**, *263*, 658. (b) Nicoud, J.-F. *Science* **1994**, *263*, 636. (c) Dhenaut, C.; Ledoux, I.; Samuel, I. W.; Zyss, J.; Bourgault, M.; Bozec, H. L. *Nature* **1995**, *374*, 339.
(2) Rikken, G. L. J. A.; Raupach, E. *Nature* **1997**, *390*, 493.
(3) (a) Kimura, T.; Goto, T.; Shintani, H.; Ishizaka, K.; Arima, T.; Tokura, Y. *Nature* **2003**, *426*, 55. (b) Yamasaki, Y; Miyasaka, S.; Kaneko, Y.; He, J.-P.; Arima, T.; Tokura, Y. *Phys. Rev. Lett.* **2006**, *96*, 207204.
(4) (a) Kumagai, H.; Inoue, K. *Angew. Chem., Int. Ed.* **1999**, *38*, 1601. (b) Minguet, M.; Luneau, D.; Lhotel, E.; Villar, V.; Paulsen, C.; Amabilino, D. B.; Veciana, J. *Angew. Chem., Int. Ed.* **2002**, *41*, 586.
(5) (a) Inoue, K.; Imai, H.; Ghalasaki, P. S.; Kikuchi, K.; Ohba, M.; Ōkawa, H.; Yakhmi, J. V. *Angew. Chem., Int. Ed.* **2001**, *40*, 4242. (b) Inoue, K.; Kikuchi, K.; Ohba, M.; Ōkawa, H. *Angew. Chem., Int. Ed.* **2003**, *42*, 4810. (c) Imai, H.; Inoue, K.; Kikuchi, K.; Yoshida, Y.; Ito, M.; Sunahara, T.; Onaka, S. *Angew. Chem., Int. Ed.* **2004**, *43*, 5618. (d) Kishine, J.; Inoue, K.; Yoshida, Y. *Prog. Theor. Phys.* **2005**, *159*, 82.
(6) (a) Ohba, M.; Ōkawa, H. *Coord. Chem. Rev.* **2000**, *198*, 313. (b) Ōkawa, H.; Ohba, M. *Bull. Chem. Soc. Jpn.* **2002**, *75*, 1191. (c) Coronado, E.; Gómez-García, C. J.; Zuez, A.; Romero, F. M.; Rusanov, E.; Stoeckli-Evans, H. *Inorg. Chem.* **2002**, *41*, 4615. (d) Coronado, E.; Gómez-García, C. J.; Zuez, A.; Romero, F. M.; Waerenborgh, J. C. *Chem. Mater.* **2006**, *18*, 2670.
(7) (a) Hernández-Molina, M.; Lloret, F.; Ruiz-Pérez, C.; Julve, M. *Inorg. Chem.* **1998**, *37*, 4131. (b) Andrés, R.; Brissard, M.; Gruselle, M.; Train, C.; Vaissermann, J.; Malézieux, B.; Jamet, J.-P.; Verdaguer, M. *Inorg. Chem.* **2001**, *40*, 4633. (c) Coronado, E.; Galán-Mascarós, J. R.; Gómez-García, C. J.; Martínez-Agudo, J. M. *Inorg. Chem.* **2001**, *40*, 113. (d) Coronado, E.; Galán-Mascarós, J. R.; Martí-Gastaldo, C. *J. Mater. Chem.* **2006**, *16*, 2685.
(8) Coronado, E.; Galán-Mascarós, J. R.; Gómez-García, C. J.; Murcia-Martínez, A. *Chem.—Eur. J.* **2006**, *12*, 3484.
(9) Compound **1S**: yield, 46 mg, 59%. Anal. Calcd for $C_9H_{17}N_8O_3Mn_2$ (%): C, 27.36; H, 4.34; N, 28.36. Found: C, 27.29; H, 4.12; N, 4.12. Selected FT-IR data [ν_{CN} / cm^{-1}] using KBr disk: 2150(w), 2140, 2129. Compound **1R**: yield, 35 mg, 45%. Anal. Calcd: C, 27.36; H, 4.34; N, 28.36. Found: C, 27.04; H, 4.05; N, 28.35. Selected FT-IR data [ν_{CN} / cm^{-1}] using KBr disk: 2150(w), 2140, 2129. The valences of Mn were verified by bond-valence sum calculations and IR data. Warning: Cyanide-containing compounds are potentially toxic and should only be handled in small amounts.
(10) X-ray crystallographic data for **1S** at 243 K ($C_9H_{17}N_8O_3Mn_2$): fw = 395.16, dark-red plates (0.21 × 0.20 × 0.19 Å^3), orthorhombic, space group $P2_12_12_1$, $a = 7.531(1)$, $b = 14.291(2)$, $c = 14.920(3)$ Å, $V = 1605.7(5)$ Å^3, $Z = 4$, $D_{calcd} = 1.634$ g cm^{-3}, μ (Mo Kα) = 15.96 cm^{-1}. $R = 0.058$, $R_w = 0.084$ (for 12659 all reflections) and $R_1 = 0.032$ ($I > 2.0\sigma(I)$). X-ray crystallographic data for **1R** at 243 K ($C_9H_{17}N_8O_3Mn_2$): fw = 395.16, dark-red plates (0.28 × 0.12 × 0.05 Å^3), orthorhombic, space group $P2_12_12_1$, $a = 7.5145(5)$, $b = 14.261(1)$, $c = 14.844(1)$ Å, $V = 1590.7(2)$ Å^3, $Z = 4$, $D_{calcd} = 1.650$ g cm^{-3}, μ (Mo Kα) = 16.11 cm^{-1}. $R = 0.062$, $R_w = 0.116$ (for 13245 all reflections) and $R_1 = 0.042$ ($I > 2.0\sigma(I)$). In both cases, the position of one lattice water molecule could not be accurately determined because of incommensurate arrangement. The structure was solved by direct methods using the SIR97 program and refined on F^2 with the teXsan program.
(11) Details are given in Supporting Information.
(12) Alexander, J. J.; Gray, H. B. *J. Am. Chem. Soc.* **1968**, *90*, 4260.

JA066140B